Zhang, J., Long, Z., Liu, W., and Chen, Q. "Strategy for studying ventilation performance in factories," Accepted by *Aerosol and Air Quality Research*.

Strategy for studying ventilation performance in factories

Jie Zhang[1], Zhengwei Long[1*], Wei Liu[1, 2], Qingyan Chen[1, 2]

[1]*Tianjin Key Lab. of Indoor Air Environmental Quality Control, School of Environmental Science and Engineering, Tianjin University, Tianjin 300072, China*

[2]*School of Mechanical Engineering, Purdue University, West Lafayette, IN 47907, USA*

Abstract:

High concentrations of airborne particulate matter in factories can cause serious health problems for workers. One significant reason for these high concentrations is the poor performance of the ventilation systems in workplaces. This investigation developed a strategy that combines computational fluid dynamics (CFD) simulations and on-site measurements to study and improve the ventilation performance in factories. The CFD simulations were able to predict the flow field and particle distributions in factories with complex layouts. The corresponding on-site measurements were performed to provide boundary conditions for the CFD simulations and to obtain key data about airflow and air quality for validating the simulations. This study used the strategy to improve ventilation performance in an automotive parts factory. Three ventilation systems were studied: a roof exhaust system, combined roof exhaust and air recirculation systems, and combined roof exhaust and displacement ventilation systems. This study found that the combined roof exhaust and displacement ventilation systems provided acceptable indoor air quality and thermal comfort levels in the factory.

Keywords: Factory; Particulate matter; Ventilation; Field measurement; CFD

[*] Corresponding author. Tel: 86-151-2245-8261; Fax: 86-22-2740-9500

E-*mail address*: longzw@tju.edu.cn

INTRODUCTION

Manufacturing processes in factories often produce a large number of particles. Very often these particles enter the air in occupied zones, with a potentially serious impact on the health of workers (Hsu et al., 2012). Zhou et al. (2007) found that among 176 factories in Shenzhen, China, 113 ontained toxic hazards and 98 had excessive quantities of particulate matter. He et al. (2012) investigated hazardous materials in 88 workplaces in Changsha, China, and found that concentrations of particulate matter in nearly half of the workplaces exceeded the exposure limits. Ren et al. (2012) examined 5,913 samples of particulate matter from 580 factories in Haidian District, Beijing, China, from 2006 to 2010. The results showed that 11.5% of the samples did not meet air quality standards. Long-term exposure to particulate matter may cause asthma, heart disease, laryngeal cancer, bronchial hyper-responsiveness, and lung cancer (Buonanno et al., 2011; Chen et al., 2007; Davidsona et al., 2005; Kazerouni et al., 2000; Judy et al., 2013). Thus, it is very important to study airborne particulate matter in factories.

Particle concentration in factories is significantly influenced by ventilation systems (Chien et al., 2007; Lai and Wong, 2010). Effective ventilation systems can reduce the concentration of airborne particles to acceptable levels and can also maintain a thermally comfortable indoor environment (Caputo and Pelagagge 2009; Kim et al. 2014). A general method of investigating ventilation performance and thermal comfort in factories is computational fluid dynamics (CFD). But CFD simulations often use many assumptions, so it is essential to obtain key data about airflow and air quality by means of on-site measurements for validating the CFD results. Russo et al. (2008) and Makhoul et al. (2012, 2013) developed a detailed CFD model to simulate the airflow and particle distribution in a chamber with a seated thermal manikin. On site measurements were conducted for obtaining the boundary conditions and validating the CFD model. Their results proved that the method of combining CFD simulation with on-site measurements was appropriate to investigate the ventilation performance. However, the challenge is that the factories are far more complicated than the chamber for both modeling and measurement. Moon et al. (2005, 2006) used CFD to investigate the performances of the jet fans and a displacement ventilation system in a welding factory. However, they did not have experimental data to validate their results. Wang et al. (2012) used an additional personal ventilation system to improve ventilation performance in a factory with a displacement ventilation system, but the agreement between the computed results and on-site measurements was poor because of many unknown factors. Rohdin and Moshfegh (2007) studied ventilation performance by using different CFD models in a packaging factory and demonstrated that the RNG k-ε model was the best. However, their boundary conditions were relatively simple, which may not be typical in factories. Rohdin and Moshfegh (2011) also used this method to compare the performances of mixing and displacement ventilation systems in a shake-out factory with a complex particle emission source. Although the model was able to accurately predict the air velocity and temperature, it could not predict the particle concentrations in regions close to the inlets and outlets because of simplifications in grouping the machines in the space. Huang et al. (2014) employed the Lagrangian model to predict particle transmission in an enzyme factory and obtained satisfactory results for particle concentration, air velocity, and air temperature. Because there was only one source, they were able to estimate the particle source strength from the particle concentration. If there had been multiple sources emitting particles with variable rates, the method has not been used. Because of the complex nature of thermo-fluid boundary conditions in factories, the approaches discussed above differ greatly from one another. Each situation is unique, making it difficult to improve the performance of ventilation systems. It is necessary to develop a reliable strategy for studying and improving ventilation performance in factories.

This paper reports our approach of using a combination of CFD modeling with limited on-site measurements to study the ventilation performance in factories. Using several examples, this investigation shows that our strategy should help designers to streamline their ventilation system design process while maintaining acceptable indoor environmental quality in factories.

METHODS

Previous studies (Huang et al., 2014; Moon et al., 2005, 2006; Rohdin and Moshfegh, 2007, 2011; Wang et al., 2012) have shown that CFD is a powerful tool for studying ventilation performance in factories. The tool is inexpensive and can handle most of the thermo-fluid boundary conditions encountered in real-life scenarios. However, CFD uses approximations, so that the simulated results should be validated with experimental data. Because validation requires only a few key data points, it is unnecessary to measure air distribution with a high resolution, which can be costly in a factory.

Numerical models

To simulate turbulent airflow in a factory, this investigation used CFD based on the Reynolds-averaged Navier Stokes equations with the renormalization group RNG k–ε model (Launder and Spalding, 1972). The general form of the governing equations can be written as:

$$\frac{\partial(\rho\varphi)}{\partial t} + div(\rho u\varphi) = div(\Gamma grad\varphi) + S \tag{1}$$

where φ represents the general variables, mass conservation (φ = 1), the three components of air velocity ($\varphi = u_j$ with j = 1, 2, 3), turbulence kinetic energy *(φ = k)*, turbulence dissipation rate (φ = ε), and air temperature ($\varphi = T$); t the time; ρ the air density; Γ the effective diffusion coefficient; and S the source term.

This study used a commercial CFD program, ANSYS Fluent (Ansys, 2009), to solve the discretized form of Eq. (1) by the finite volume method under steady-state conditions. The investigation used the RNG k-ε model for modeling turbulent flow and the standard wall functions (Ansys, 2009). The equations were discretized with the second-order upwind scheme, and pressure and velocity were coupled by the SIMPLE algorithm (Patankar, 1980). Boundary conditions for airflow field included the airflow and temperature profiles. Because the flow rates of the air conditioning systems were fixed, the mass flow rate boundary was applied. For the turbulence intensity at the supplies, we can measure the air velocity near the inlets as long time as possible and calculate it by the following equations:

$$I \equiv u^{'}/U \tag{2}$$

Where I represents the turbulence intensity; u′ the root-mean-square of the turbulent velocity fluctuations; U the mean velocity. u′ can be calculated by:

$$u^{'} \equiv \sqrt{\frac{1}{3}\left(u_x^{'2} + u_y^{'2} + u_z^{'2}\right)} \tag{3}$$

Where $u_x^{'}$, $u_y^{'}$, $u_z^{'}$ are the air velocity fluctuations in x, y, and z direction, respectively. U can be calculated by:

$$U \equiv \sqrt{U_x^2 + U_y^2 + U_z^2} \tag{4}$$

Where U_x, U_y, U_z are the mean air velocities in x, y, and z direction, respectively. In addition, if the on-site measurements are not available, Zhang et al. (2012) suggested the turbulence intensity of 10% is applicable for general air inlets. The opened doors used velocity inlet boundary with the air velocity profile obtained from on-site measurement. Because the pressure determined the exhaust flow rate, the corresponding pressure outlet was used for the exhausts. For the thermal boundaries, fixed temperatures were applied at envelops, equipment and ducts. The air was treated as incompressible fluid. The Boussinesq approximation was used to consider the buoyancy effect. The simulation could be considered converged if the air velocity, turbulence intensity and temperature at key locations varied very little and the net mass and energy balance rates were both less than1‰. To predict the steady-state particle concentration distribution in a factory, both the Eulerian and Lagrangian methods can be used (Zhao et al., 2008, 2004). Because Zhang and Chen (2007) found that the Lagrangian approach was more accurate than the Eulerian approach in predicting particle dispersion in an indoor environment, this study used the Lagrangian approach. This approach calculates individual trajectories by solving the momentum equation:

$$\frac{du_p}{dt} = F_D(u - u_p) + \frac{g_x(\rho_p - \rho)}{\rho_p} + F_x \tag{5}$$

where u_p is the particle velocity, t the time, F_D the inverse of the relaxation time, u the air velocity, g_x the acceleration of gravity, ρ_p the particle density, ρ the air density, and F_x the additional forces. The term on the left-hand side of Eq. (2) represents inertial force; the first term on the right-hand side represents drag force; the second term gravity and buoyancy forces; and the last term includes Saffman's lift force, force caused by Brownian motion, etc. When the particle diameter is greater than 0.5 μm, the gravity and drag forces are the most important. The rest of the forces are negligible, so they were not considered in our investigation.

As the Lagrangian approach uses stochastic particle tracking that may introduce some uncertainties into the concentration calculation, a sufficient number of trajectories should be tracked. Zhang (2005) indicated that 50,000 samples were needed for only 7500 cells. Thus, the grid size should be large enough to ensure the stability of the solutions. On the other hand, as the volume fraction of particles is small in a factory, the impact of discrete particle phase to continuum fluid phase can be neglected and the force interaction between the two phases is only considered from fluid phase to discrete phase by using the discrete random walk (DRW) model (Ansys, 2009; Zhang and Chen, 2006). The model predicts the particle dispersion due to turbulence by calculating eddies with a Gaussian distributed random velocity fluctuation and a time scale. This investigation used the DRW model.

Not only does turbulence have an impact on particle motion, but particles can be deposited on or reflected by rigid surfaces. Hinds (1982) found that particles did not have enough energy to rebound from a surface, so they were most often attached to the surface. Zhang and Chen (2006) suggested that the use of a small restitution coefficient would be more reasonable than treating the particles as completely trapped. The current study used the coefficient determined by Zhang and Chen (2006). The particle emission time was set long enough to ensure the particle is well mixed in the computational domain. The particle field was considered converged if the particle concentration at the breathing height of 1.5 m above the floor was stabilized.

To create a CFD model that can accurately simulate the airflow and particle field in a factory, a well-studied grid strategy should be performed before running the simulation progress. Gambit 2.4.6 was used to generate the grid. We conducted the grid independence study and chose the best performance one by considering both the accuracy and the computational efficiency. As the factories had significantly different geometric scales, unstructured tetrahedral grid with coarse globe size was used.. For the grids at small size geometry positions such as the air supply inlets, outlets and the particle emission outlets, a fine size with 10% of the length of the inlets and outlets were chosen. To reduce the maximum skewness of the mesh, the grid size gradually expanded to that of the main domain. In addition, the near wall grid was refined in order to use standard wall function, which requires that the near wall averaged y+ should be larger than 30.

On-site measurements

CFD simulations require information about thermo-fluid boundary conditions, and validation of CFD results requires key airflow and particle concentration data. The boundary conditions in a factory typically consist of wall temperatures, airflow rates, turbulence intensity and temperatures from ventilation systems, infiltration through the building envelope, particle diameter and strength from their sources, etc. Validation requires only a small number of data points from typical locations in the factory. This investigation used various instruments for the measurements, as shown in Table 1. Further details are provided in Section 3.

Ventilation performance evaluation

In order to evaluate the performance of the ventilation systems in a factory, this study applied the ventilation effectiveness equation (Mats, 1981):

$$\eta = \frac{c_e - c_s}{c - c_s} \tag{6}$$

where c_e is the average particle concentration in the local exhaust air (kg/m^3), c the average particle concentration at breathing level (kg/m^3), and c_s the average particle concentration in the supply air (kg/m^3). The higher the ventilation effectiveness is, the better the performance of the ventilation system.

CASE DESCRIPTION

The research method outlined above was used to study air quality, thermal comfort, and ventilation performance in an automotive parts factory. Figure 1 is a schematic of the factory with dimensions of 206 m long, 90 m wide and 8 m high. Door 1, with an area of 5.2 m^2, was always open to the reception hall. Doors 2, 3, and 5 were opened frequently, while Door 4 was seldom opened. Doors 6 and 7 on the east wall were connected to another building. Outdoor air could flow into the factory through all these door openings. The roof had eight skylights across the building width, with significant cracks as illustrated in Fig. 2. The factory had three types of ventilation system: air recirculation with filters, displacement ventilation, and roof exhausts, as depicted in Fig. 3. The air recirculation system supplied conditioned air downward from a location at the mid-height of the factory. Although this system had filters, their efficiency in removing fine particles was negligible. The displacement ventilation system supplied 100% outdoor air horizontally near the floor along the south wall, and the exhaust ducts for this system were on the opposite partition wall at a height of 6.0 m above the floor. In addition, there were seven groups of exhausts evenly distributed across the roof.

The manufacturing processes in this factory involved cutting, twisting, grinding, quenching, and cleaning, which produced different numbers and sizes of particles and different amounts of heat. The factory had five production regions with hundreds of machines, which were simplified as arrays of rectangular boxes shown in Fig.1 and Fig. 4. Although our simulation was performed for the whole factory, we just showed the airflow and particle field of the region enclosed by the yellow lines in Fig. 1 and represented by the pink boxes in Fig. 4 since the particle concentration at that region was the highest.

For predicting the air velocity and particle concentration distributions in this factory, thermo-fluid boundary conditions needed to be measured as inputs for CFD. The infrared camera specified in Table 1 was used to measure the interior surface temperatures of the building envelope and the exterior surface temperatures of the ventilation ducts and machines. A hot-wire anemometer (Model TSI-8386) was used to measure the velocity and temperature of the supply and return air in the ventilation systems and of the airflow through the door openings. Because Doors 2, 3, and 5 opened and closed frequently, the airflow rates were not constant. The flow rates through these doors were the mean rates determined by the opening frequency. The rate of infiltration through cracks in the skylights was determined by (General Administration of Quality Supervision, Inspection and Quarantine of the People's Republic of China and Standardization Administration of the People's Republic of China, 2008):

$$V = nLl \tag{7}$$

where V is the infiltration rate (m^3/s), n the correlation coefficient, L the infiltration per linear length under a 10 Pa pressure difference (m^3/s), and l the effective length of the skylights (m).

The factory had roof exhausts as shown in Fig. 1. The airflow rate through the exhausts was determined by a mass balance with the air supply from the ventilation systems, the airflow through the door openings, and the infiltration through the building envelope. The particle concentrations at the sources were measured by an aerosol monitor (Model TSI-8530 Dustrak). Measurements of air velocity and area at the source outlets allowed the particle generation rate from the sources to be determined. The particle diameters were measured by an aerodynamic particle sizer (Model TSI-3321).

RESULTS

Validation of the CFD model

To validate the CFD model, this study performed CFD simulations with the measured thermo-fluid boundary conditions. The simulated air velocity, temperature and particle concentrations were then compared with the measured data at several key locations in the factory. The experimental data was obtained on-site on a winter day.

Table 2 summarizes the boundary conditions used in the CFD simulations. The surface temperature was averaged because it was not uniform. The largest standard deviation (SD) of the average temperature was ±1.3 ºC. All the airflow rates of the air conditioning systems were obtained from the provided data by the operators, so the SDs were not available. This study set the turbulence intensity of 10% to the supply inlets of the air recirculation systems (Zhang et al. (2012)). But for the displacement ventilation system, we measured the air velocity at the inlets for 5 min and calculated the turbulence intensity by Eqs. (2)-(4). The effective length of the skylights was 603.2 m. Under the assumptions that L was equal to 1.7×10^{-3} m^3/s and n was equal to 1, we used Eq. (7) to estimate an air infiltration rate of 8.1 m^3/s. The relative errors of the velocity of the opened doors were all lower than 10%. By performing a mass balance, this investigation found that the airflow rate through the roof exhausts was 123.9 m^3/s. This study also used an averaged strength for the particle sources from the machines with the SD of $\pm8.9\times10^{-8}$ kg/s. The aerodynamic diameters of the particles were found to be in the range of 0.5-0.8 μm. Our simulations used the diameter of the highest concentration of 0.7 μm. The velocity of particles injected from the equipment was the averaged value with ±0.02 deviation. The measurements for validation of the CFD results were performed at breathing level of 1.5 m above the floor in 10 key locations, shown as A1-A5 and B1-B5 in Fig. 5. Figure 6 shows that, in most locations, the CFD results were close to the measured data or within the uncertainty range of the data. Because of the complex airflow pattern, uncertainties in the measurements, and approximations in the CFD simulation, a perfect agreement between the CFD results and the experimental data is unrealistic and may never be achieved. Thus, we consider the differences to be acceptable and the CFD model to have been validated.

Analysis of ventilation system performance

The factory had multiple ventilation systems, and they may have counteracted one another so that the airflow was not organized. Because of the poor air distribution and low air change rate, the particle concentration in the factory exceeded the exposure limit of 0.5 mg/m^3 (shown in Fig.6) as specified by the national standard (National Occupation Health Standard of the People's Republic of China, 2007). This factory used three ventilation systems: a roof exhaust system, a recirculation system, and a displacement ventilation system. The roof exhaust system was intended to remove particulate pollutants, and the other two were intended to control the indoor air temperature at an acceptable level for the workers and also to improve ventilation effectiveness.

In this section, we discuss the use of the validated CFD model to evaluate the performance of these systems in the factory. The evaluation was conducted for the following cases:

1. the roof exhaust system only;
2. a combination of the roof exhaust and air recirculation systems; and
3. a combination of the roof exhaust and displacement ventilation systems.

A combination of ventilation systems is necessary because a single system cannot provide an acceptable indoor environment, as evidenced by the case with only the roof exhaust system, discussed below. The three cases had the same boundary conditions, as shown in Table 2, with the exception of ventilation rate.

For the case with only the roof exhaust system, Fig. 7 presents the air velocity and particle concentration distributions in the working region illustrated in Fig. 5. As shown in Fig. 7(a), the air distribution for this case was fairly good. The strong upward air velocities were due to the roof exhaust fans and the thermal buoyancy forces from the machines. However, ventilation through the roof exhausts was limited, so the buoyant flows that reached the ceiling formed air circulation patterns in some regions. Nevertheless, the upward air movement brought contaminated air to the upper part of the factory, as illustrated in Fig. 7(b), and a large portion of the air was extracted through the roof exhausts. Fig. 7(b) also shows that, because of infiltration and door openings, the air in the perimeter of the factory was quite clean. In the vertical plane it can be clearly seen that air distribution played a very important role in ventilation effectiveness. These results also indicate that the roof exhaust system could effectively remove particles from the factory when the ventilation rate was sufficiently high.

The above analysis can be extended to the entire region. As shown in Fig. 7(c), the particle concentration distribution in the working region was high at breathing level of 1.5 m above the floor. The perimeter zone was much cleaner than the working region, again because of the airflow pattern. It seems that it would be possible to create a clean working environment in the factory by further increasing the ventilation rate through the roof exhausts. However, without a heating system, the air temperature in the factory can be very low in winter. For example, when the outdoor air temperature was -3 ^{o}C on a winter day, the indoor air temperature was measured at only 9 ^{o}C. This temperature was too low for providing an acceptable level of thermal comfort to the workers.

Our second case incorporated the air recirculation system that was used to provide heating for the workers in the factory. The heat exchangers in this system heated the air at the outlets to a temperature of 32 ºC on a winter day. Cooling coils in the system provided cooling in the summer. As shown in Fig. 3, the air was supplied in a downward direction from the air recirculation system. The airflow counter-acted the buoyant flows from the machines. Fig. 8(a) shows that the resulting airflow pattern was mainly downward. As a result, particles were trapped in the occupied area, and at breathing level of 1.5 m above the floor level the particle concentration was even higher than that with only the roof exhaust system, as shown in Fig. 8(b). One major reason for this high concentration was that the roof exhaust system could not effectively remove particles because of the poor airflow pattern. Fig. 8(c) illustrates the particle concentration distribution at breathing level of 1.5 m above the floor. The concentration in the entire region was clearly higher than that in the first case. The average particle concentration in the working region was 4.53 mg/m^3, which was 1.57 times higher than that in the first case. These results indicate that combining the air recirculation system with the roof exhaust system was not the proper approach, even though the former system improved thermal comfort in the factory.

The above results illustrate the dilemma faced by the factory: the roof exhaust system alone could provide good air quality, but thermal comfort level was low; while the combined roof exhaust and air recirculation systems improved thermal comfort, but the air recirculation system made the air quality worse. Therefore, in the third case the air recirculation system was replaced by the factory's displacement ventilation system. Displacement ventilation typically supplies air in the lower part of an indoor space at a slightly lower temperature than that of the room air. The negative buoyancy force keeps the clean air in the lower part of the factory, while the heat generated by the machines raises the air temperature to a comfortable level. However, in the factory studied, the heat from the machines was insufficient to heat the room air. The factory owner did not want to add another heating system because of the capital investment required. Therefore, the displacement ventilation system supplied warmer air of 25.3 ^{o}C to the factory. Since the air temperature was not very high, the inertial force was actually much higher than the buoyant force, and thus the clean air remained in the lower part of the factory as shown in Fig. 9(a). Because of the great width of the factory, the air from the displacement ventilation system eventually traveled upward at a point one-third of the way from the right wall. Ideally, the air should be supplied from both the left and right walls. Because there was a furnace room on the other side of the left wall, it was impossible to supply outside air from that wall. Therefore, the displacement ventilation system could improve the air quality only on the right side of this region of the factory, as shown in Fig. 9(b). Although the particle concentration was higher on the left side of the region than on the right side, Fig. 9(c) shows that the overall concentration at breathing level of 1.5 m above the floor was lower than that in the first and second cases. This lower concentration occurred because the flow from displacement ventilation assisted the flow from the roof exhaust system, creating a desirable airflow pattern. The air generally flowed upward in the entire region, as illustrated in Fig. 9(a). The average particle concentration in the working region was about 2.48 mg/m^3, which was the lowest among the three cases. In addition, the air temperature of the occupied zone could be maintained at 18.5^{o}C, which was good for the thermal comfort of the workers. It can be concluded that the combined displacement ventilation and roof exhaust systems were effective in removing particles and maintaining a comfortable thermal environment in the factory.

Table 3 further summarizes the average air temperatures and particle concentrations at breathing level of 1.5 m above the floor in the working region, and the ventilation effectiveness as calculated by Eq. (6). The third case had the best performance.

CONCLUSIONS

This study developed a strategy for studying and improving ventilation performance in factories. The strategy used on-site measurements to provide boundary conditions for the CFD simulations and to obtain key air distribution information for validating the CFD program. The validated CFD program was then used to study the ventilation effectiveness and thermal comfort under different ventilation- system scenarios.

By applying the strategy to the evaluation of particle concentration, air velocity, and air temperature in an automotive parts factory, this study found that using only a roof exhaust system would make it difficult to heat the air in the winter and would result in a low level of thermal comfort. With the addition of an air recirculation system with heating/cooling coils, the downward air supply would counteract the upward buoyant flow so that particles would be trapped in the working region. The air quality declined, although thermal comfort improved. The best scenario was to replace the air recirculation system with a displacement ventilation system. The combination of roof exhaust and displacement ventilation systems can greatly improve air quality and maintain thermal comfort at acceptable levels.

ACKNOWLEDGMENTS

The research presented in this paper was financially supported by the National Natural Science Foundation of China though Grant No. 51106105.

REFERENCES

Ansys. (2009). *ANSYS Fluent Theory Guide*, ANSYS, Inc.

Buonanno G, Morawska L and Stabile L. (2011). Exposure to welding particles in automotive plants. *J. Aerosol Sci.* 42: 295-304.

Caputo A.C and Pelagagge P.M. (2009). Upgrading mixed ventilation systems in industrial conditioning. *Appl. Therm. Eng.* 29: 3204-3211.

Chen M.R, Tsai P. J, Chang C.C, Shih T.S, Lee W.J. and Liao P.C. (2007). Particle size distributions of oil mists in workplace atmospheres and their exposure concentrations to workers in a fastener manufacturing industry. *J. Hazard. Mater*. 46: 393-398.

Chien C. L., Tsai C. J., Ku K. W. and Li S. N. (2007). Ventilation Control of Air Pollutant during Preventive Maintenance of a Metal Etcher in Semiconductor Industry. *Aerosol Air Qual. Res.* 4: 469-488.

Davidsona C. I., Phalenb R. F. and Solomonc P. A. (2005). Airborne Particulate Matter and Human Health: A Review. *Aerosol Sci. Tech.* 8: 737-749.

General Administration of Quality Supervision, Inspection and Quarantine of the People's Republic of China and Standardization Administration of the People's Republic of China. (2008). *Graduation and test methods of air permeability,watertightness,wind load resistance performance for building external windows and doors*, GB/T 7106-2008.

Huang C.H. and Lin P.Y. (2014). Influence of spatial layout on airflow field and particle distribution on the workspace of a factory. *Build. Environ.* 71: 212-222

He J, Peng Y.Q. and He L.P. (2012). Analysis of results in detection of harmful factors in industrial enterprises in Changsha in 2011. *China Health Care and Nutrition* 8: 2285-2286.

Hinds W.C. (1982). *Aerosol Technology: Properties, Behavior, and Measurement of Airborne Particles,* Wiley-Interscience, New York.

Hsu H. I., Chen M. R., Wang S. M., Chen W. Y., Wang Y. F., Young L. H., Huang Y. S., Yoon C. S. and Tsai P. J. (2012). Assessing Long-Term Oil Mist Exposures for Workers in a Fastener Manufacturing Industry Using the Bayesian Decision Analysis Technique. *Aerosol Air Qual. Res.* 12: 834–842.

Kim K. Y, Kob H. J., Kimb H. T., Kima Y. S., Roha Y. M. and Kim C. N. (2007). Effect of ventilation rate on gradient of aerial contaminants in the confinement pig building. *Environ. Res.* 3: 352–357.

Kazerouni N, Thomas T.L, Petralia S.A. and Hayes R.B. (2000). Mortality among workers exposed to cutting oil mist: Update of previous reports. *Am. J. Ind. Med.* 38: 410–416.

Lai A. C. K. and Wong S. L. (2010). Experimental Investigation of Exhaled Aerosol Transport Under Two Ventilation Systems. *Aerosol Sci. Tech.* 6: 444-452.

Launder B.E. and Spalding D.B. 1972. *Lectures in Mathematical Models of Turbulence,* Academic Press, New York.

Makhoul A., Ghali K., Ghaddar N. and Chakroun W. (2013a). Investigation of particle transport in offices equipped with ceiling-mounted personalized ventilators. *Build. Environ.* 63: 97-107.

Makhoul A., Ghali K. and Ghaddar N. (2013b). Desk fans for the control of the convection flow around occupants using ceiling mounted personalized ventilation. *Build. Environ.* 59: 336-348.

Moon J.H, Heo J.H, Moon S.J. and Lee J.H. Improvement of indoor air environment in a large welding factory by displacement ventilation. Proc. 27th AIVC and 4th Epic Conference, "Technologies and Sustainable Policies for a Radical Decrease of the Energy Consumption in Buildings," Lyon, France, 2006.

Moon J.H, Lee T.G, Lee J.H. and Choi CH. (2005). Evaluation of the performance of the ventilation system in the large welding working place. *Proceedings:Indoor Air*. 3318-3322.

Mats S. (1981). What is ventilation efficiency? *Build. Environ.* (2): 123-135.

National Occupation Health Standard of the People's Republic of China. (2007). *Occupational exposure limits for hazardous agents in the workplace. Part 1: Chemical hazardous agent*, GBZ 2.1-2007.

Patankar S.V. (1980). *Numerical Heat Transfer and Fluid Flow*, Hemisphere Publishing Co, Washington.

Ren Y.D, Jia G, Fang L.Y, Li H.S, Yu J.Y, Xiong Y.J. and Fang H. (2012). Occupational hazards monitoring and occupational health status of workers in industrial enterprises in Haidian District of Beijing City during the period of 2006-2010. *Occupation and Health*. 3: 290-292.

Rohdin P. and Moshfegh B. (2011). Numerical modeling of industrial indoor environments: A comparison between different turbulence models and supply systems supported by field measurements. *Build. Environ.* 11: 2365-2374.

Russo J. S., Dang T. Q. and Khalifa H. E. (2009). Computational analysis of reduced-mixing personal ventilation jets. *Build. Environ.* 8: 1559-1567.

Rohdin P. and Moshfegh B. (2007). Numerical predictions of indoor climate in large industrial premises. A comparison between different k-ε models supported by field measurements. *Build. Environ.* 11: 3872-3882.

Wendt J. K., Symanski E., Stock T. H., Chan W. and Du X. L. (2014). Association of short-term increases in ambient air pollution and timing of initial asthma diagnosis among medicaid-enrolled children in a metropolitan area. *Environ. Res*. 131: 50–58.

Wang H.Q, Huang C.H, Liu D, Zhao F.Y, Sun H.B, Wang F.F, Li C, Kou G.X. and Ye M.Q.

(2012). Fume transports in a high rise industrial welding hall with displacement. *Build. Environ.* 52: 119-128.

Zhao B, Yang C, Yang X. and Liu S. (2008). Particle dispersion and deposition in ventilated rooms: Testing and evaluation of different Eulerian and Lagrangian models. *Build. Environ.* 43: 388-397.

Zhang J., Fu H.M., Liu X.Y., Li Y. (2012). Impact of Turbulence Intensity on the Air Flow around Human Body and Thermal Comfort. Heating, Ventilating and Air conditioning, 40(261):1-5.

Zhou J, Jiang L.X. and Zhang. X.J. (2007). Determination of the poisonous and hazardous factors in the worksites of the enterprises of Futian District. *Occupation and Health.* 4: 256-257.

Zhang Z. and Chen Q.Y. (2007). Comparison of the Eulerian and Lagrangian methods for predicting particle transport in enclosed spaces. *Atmos. Environ.* 25: 5236-5348.

Zhang Z. and Chen Q.Y. (2006). Experimental measurements and numerical simulations of particle transport and distribution in ventilated rooms. *Atmos. Environ.* 40: 3396-3408.

Zhang Z. (2005). *A study on transport and distribution of indoor particulate matter*. Master thesis: Purdue University.

Zhao B, Zhang Y, Li X, Yang X. and Huang, D. (2004). Comparison of indoor aerosol particle concentration and deposition in different ventilated rooms by numerical method. *Build. Environ.* 39: 1-8.

Table Captions

Table 1 Instruments used for on-site measurements

Table 2 Measured thermo-fluid boundary conditions in the factory

Table 3 The performance of the three ventilation-system cases

Table 1 Instruments used for on-site measurements

Instruments	Parameter measured	Range	Accuracy
Vario CAM infrared camera	Surface temperature	0-100 °C	±1.5 °C
TSI-8386 hot-wire anemometer	Air velocity and air temperature	0-50 m/s −10-60 °C	±0.015 m/s ±0.3 °C
TSI-8530 DustTrak particle monitor	Particle mass concentration	0.01-400 mg/m^3	±0.001mg/m^3
TSI-3321 aerodynamic particle sizer	Particle diameter	0.5-20 μm	N/A*

*N/A means not applicable.

Table 2 Measured thermo-fluid boundary conditions in the factory

Parameters	Boundaries	Value (SD)
Surface temperature (ºC)	Mean interior wall surfaces	20.5 (±1.1)
	Floor	19.4 (±0.5)
	Roof	21.7 (±1.3)
	Mean machine surfaces	21.3 (±0.9)
	Air recirculation ducts	32.0 (±0.5)
Air recirculation systems	System 1 air supply flow rate (m^3/s)	72.2 (N/A)*
	System 1 air supply turbulence intensity (%)	10% (N/A)
	System 1 air supply temperature (ºC)	32.0 (±0.5)
	System 2 air supply flow rate (m^3/s)	93.3 (N/A)
	System 2 air supply turbulence intensity (%)	10% (N/A)
	System 2 air supply temperature (ºC)	32.0 (±0.5)
	System 3 air supply flow rate (m^3/s)	93.3 (N/A)
	System 3 air supply turbulence intensity (%)	10% (N/A)
	System 3 air supply temperature (ºC)	32.0 (±0.5)
Displacement ventilation system	Air supply flow rate (m^3/s)	30.6 (N/A)
	Air exhaust flow rate (m^3/s)	20.0 (N/A)
	Air supply turbulence intensity (%)	8% (0.7%)
	Air supply temperature (ºC)	25.3 (±0.3)
Air infiltration (m^3/s)	Skylights	8.1 (N/A)
	Doors 2, 3, and 5 (frequently open)	3.9 (±0.3)
	Doors 1, 6, and 7 (usually open)	101.3 (±3.5)
Machines	Mean particle generation rate for each machine (kg/s)	3.30×10^{-7}($\pm8.9\times10^{-8}$)
	Mean aerodynamic diameter for each machine (μm)	0.70 (N/A)
	Mean particle injection velocity (m/s)	0.15 (±0.02)

*N/A means not applicable.

Table 3 The performance of the three ventilation-system cases

Ventilation systems	Average temperature (°C)	Average Particle Concentration (mg/m^3)	Ventilation effectiveness (%)
Roof exhaust system	9.0	2.89	38.1
Roof exhaust and air recirculation systems	25.7	4.53	12.7
Roof exhaust and displacement ventilation systems	18.5	2.48	40.3

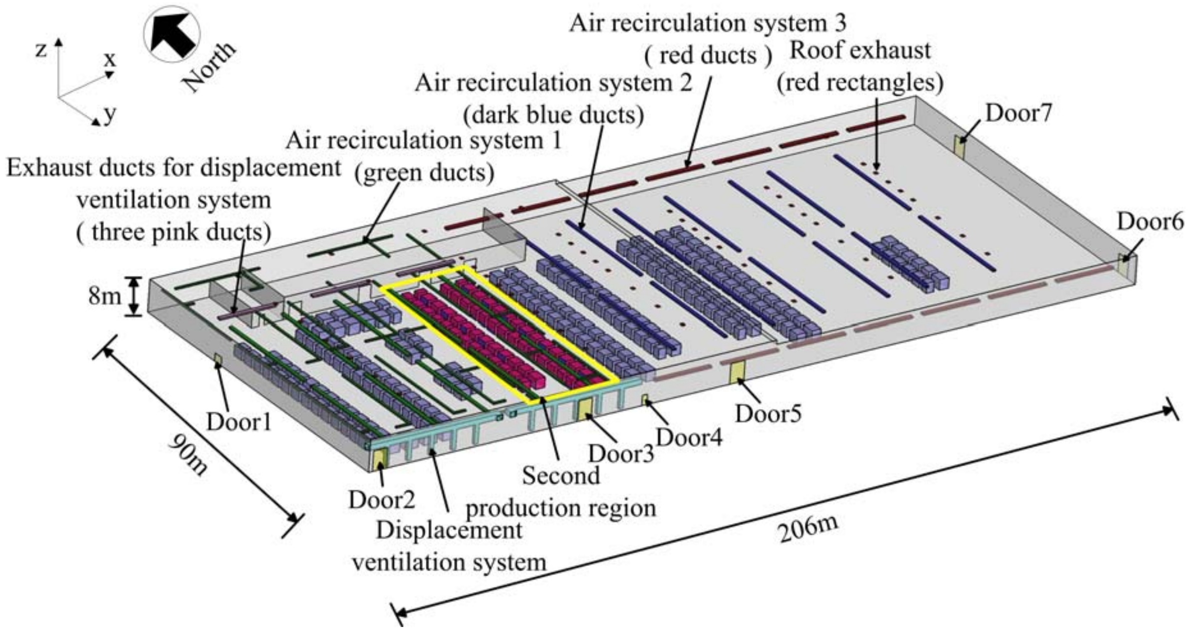

Fig. 1. Schematic of the automotive parts factory, where yellow lines indicate the region investigated in this study.

Fig. 2. Interior view of the skylights.

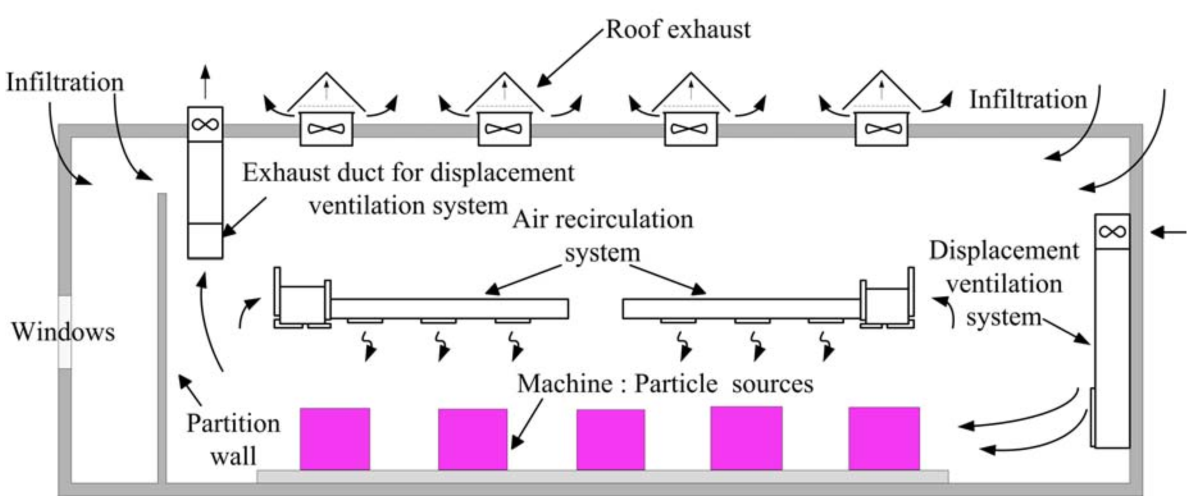

Fig. 3. Schematic view of the main processes in the automotive parts factory.

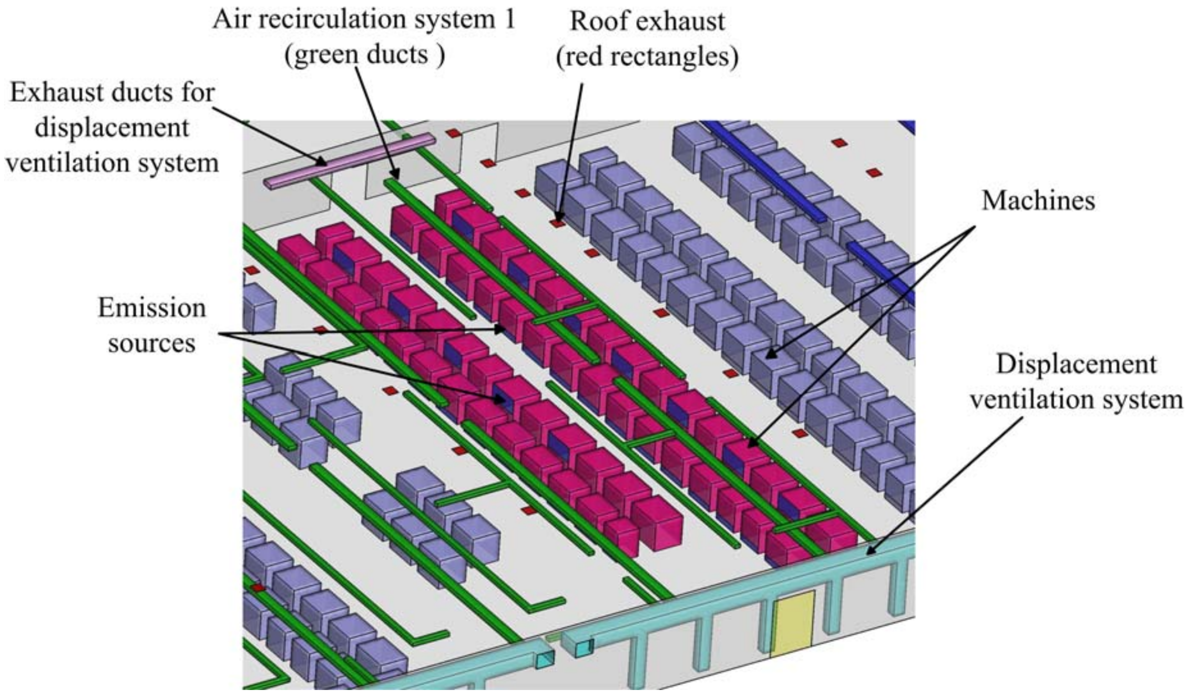

Fig. 4. Enlarged view of the production region studied.

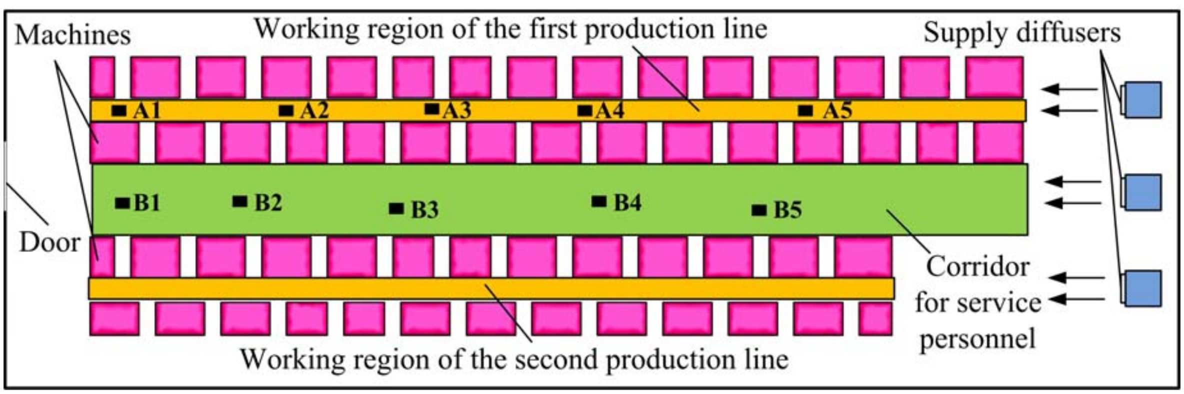

Fig. 5. The locations selected for measuring air velocity and particle concentration at breathing level of 1.5 m above the floor in the second production region of the automotive parts factory.

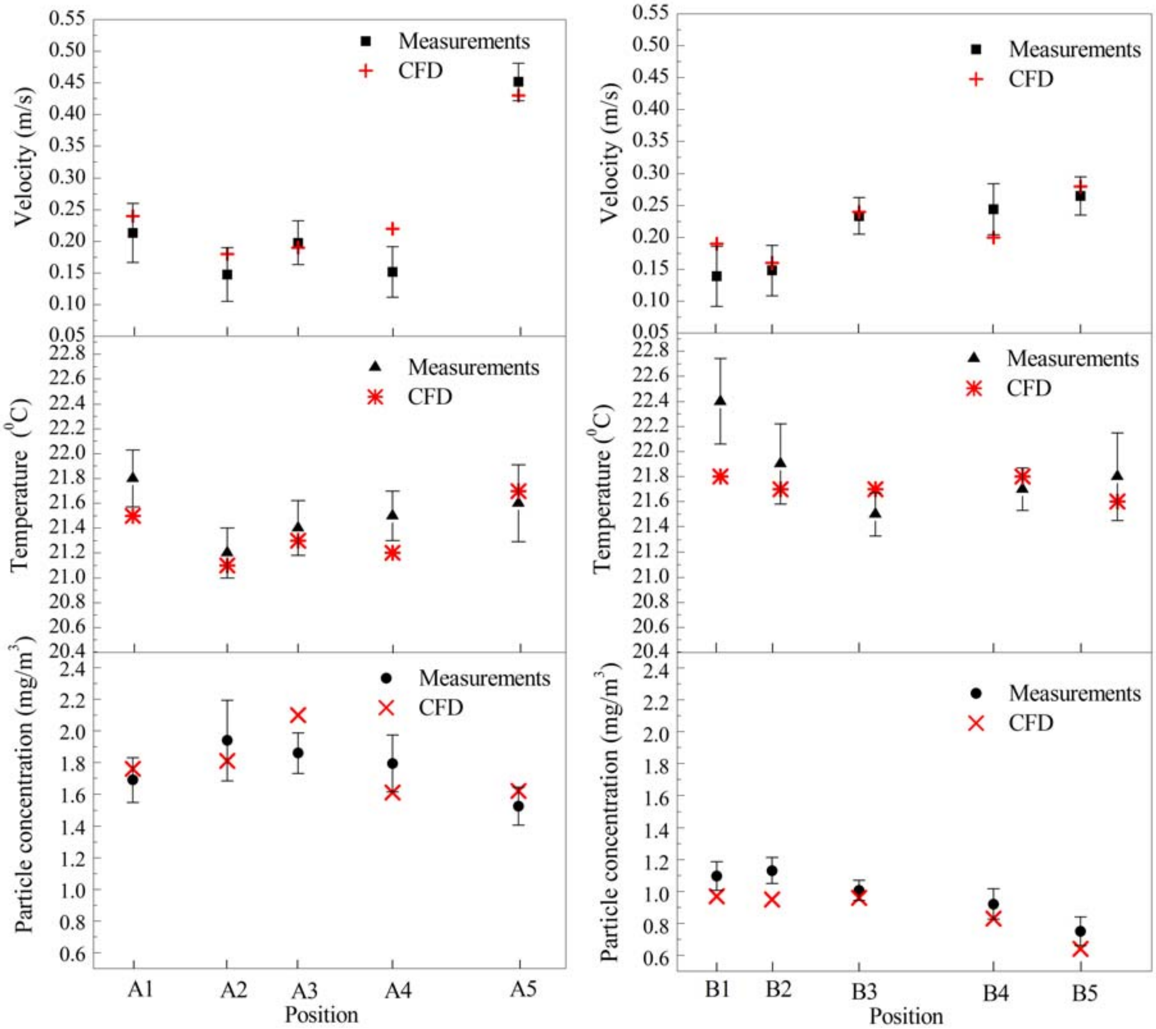

Fig. 6. Comparison of the simulated air velocity, temperature and particle concentration with the experimental data at (a) A locations and (b) B locations.

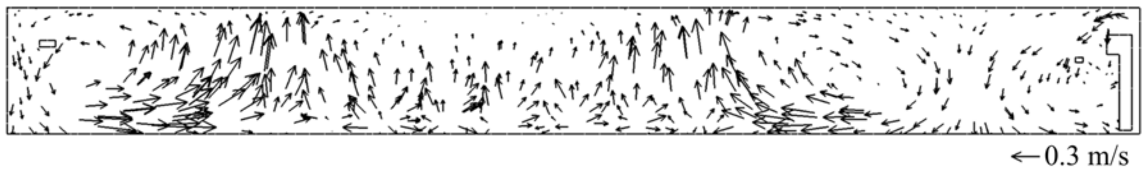

(a)

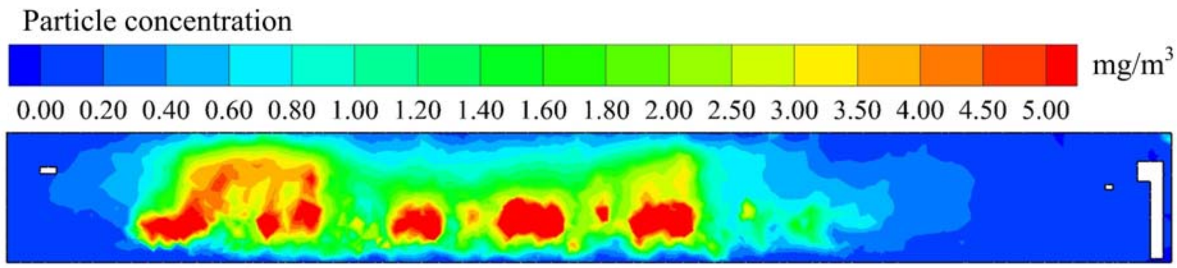

(b)

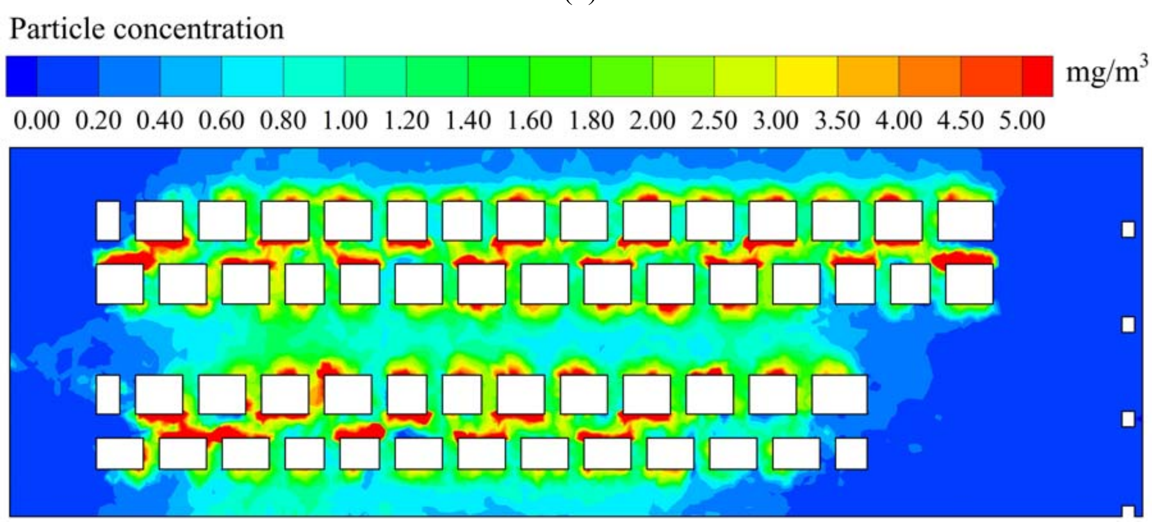

(c)

Fig. 7. Distributions in the case with only the roof exhaust system: (a) air velocity vectors ; (b) particle concentration on the middle vertical plane in the working region of the second production line shown in Fig. 5; (c) particle concentration at breathing level of 1.5 m above the floor in the region shown in Fig. 5.

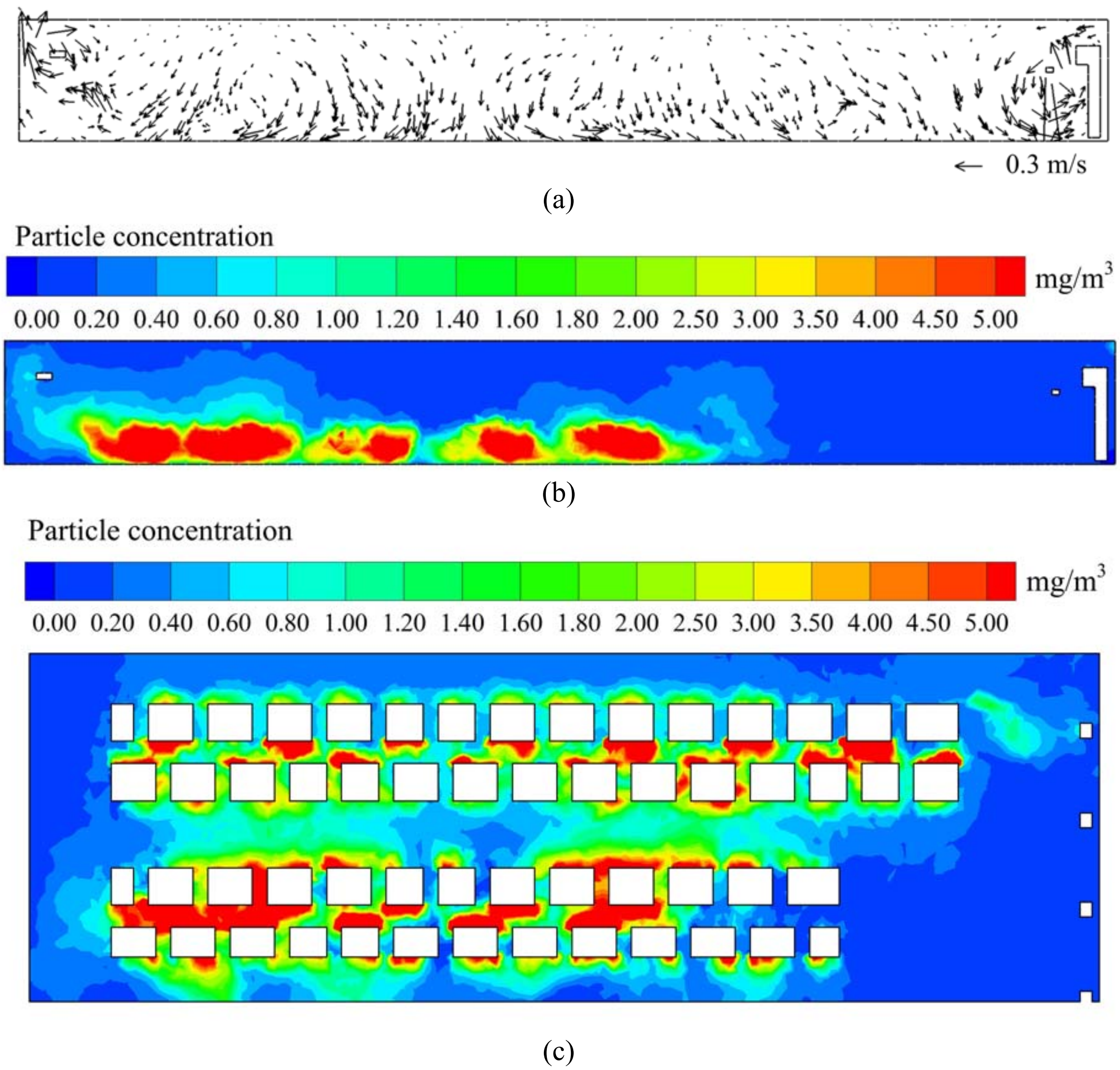

Fig. 8. Distributions in the case with the roof exhaust system and air recirculation system: (a) air velocity vectors; (b) particle concentration on the middle vertical plane in the working region of the second production line shown in Fig. 5; (c) particle concentration at breathing level of 1.5 m above the floor in the region shown in Fig. 5.

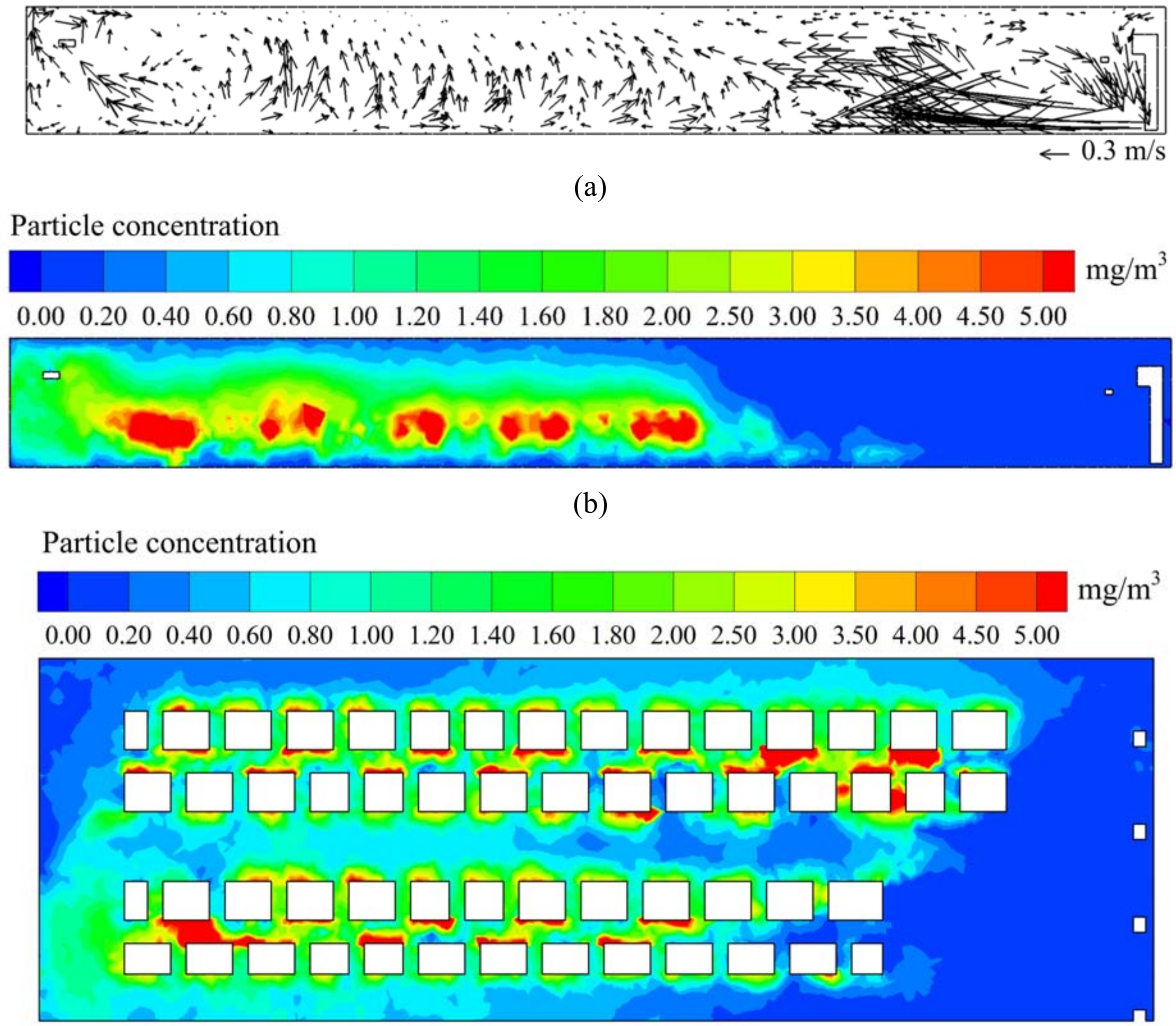

(c)

Fig. 9. Distributions in the case with the roof exhaust system and the displacement ventilation system: (a) air velocity vectors; (b) particle concentration on the middle vertical plane in the working region of the second production line shown in Fig. 5; (c) particle concentration at breathing level of 1.5 m above the floor in the region shown in Fig. 5.